

Performance Analysis of MIMO K -user Interference Channels with Hardware Impairments

Mohammad Soleymani*, *Student Member, IEEE*, Peter J. Schreier*, *Senior Member, IEEE* and Ignacio Santamaria[†] *Senior Member, IEEE*

Abstract

Next generation of wireless systems will employ many antenna branches with low-cost devices and hence, may suffer from severe hardware impairments (HWI) like I/Q imbalance, phase noise, etc. With I/Q imbalance, the received signal is a widely linear transformation of the transmitted signal and noise. Thus, the effective noise may be improper, which means that its real and imaginary parts are not independent and identically distributed. Improper Gaussian signaling (IGS) can improve system performance with improper noise and/or improper interference. This paper studies IGS for multiple-input, multiple-output (MIMO) K -user interference channels (IC) with imperfect devices in terms of two performance metrics: achievable rate and energy efficiency (EE). We also define an optimization framework for interference-limited systems when treating interference as noise. This framework obtains a stationary point of any optimization problem in which either the objective function and/or constraints are linear functions of rates. These include the optimization of the rate region, the sum-rate, the EE region, or the global EE, among others. Our numerical results show that IGS can improve the performance of MIMO K -user IC with HWI and I/Q imbalance, where its benefits increase with K and the imbalance level and decrease with the number of antennas.

Index Terms

*Mohammad Soleymani and Peter J. Schreier are with the Signal and System Theory Group, Universität Paderborn, Germany, <http://sst.upb.de> (emails: {mohammad.soleymani,peter.schreier}@sst.upb.de).

[†]Ignacio Santamaria is with the Department of Communications Engineering, University of Cantabria (email: i.santamaria@unican.es).

Achievable rate region, convex/concave procedure, energy efficiency, generalized Dinkelbach algorithm, hardware impairments, improper Gaussian signaling, interference channel, majorization-minimization, MIMO systems.

I. INTRODUCTION

Wireless communication devices are never completely ideal in practice, which can significantly degrade the system performance especially when the hardware non-idealities are not adequately modeled and accounted for the system design. The impact of hardware imperfections has become even more important in modern wireless communication systems. In particular, millimeter wave (mmW) and wideband communications, which are main trends for 5G and beyond communication systems, may severely suffer from hardware nonidealities and impairments [1]. In general, hardware impairments (HWI) may occur due to imperfections such as quantization noise, phase noise, amplifier nonlinearities, and I/Q imbalance [2]–[20].

In addition to hardware nonidealities, communication systems may suffer from strong interference because modern wireless communication systems are mostly interference-limited. Thus, interference management techniques will play a key role in next generations of wireless communications such as 5G [21]. In the last decade, the use of improper Gaussian signaling (IGS) techniques have been proposed and extensively studied as an interference-management technique [4], [22]–[39]. The real and imaginary parts of complex improper signals are correlated and/or have unequal powers, for a full treatment of improper signals the reader is referred to [40]–[42].

A. Related work

The impact of hardware nonidealities has been studied in various scenarios in [2]–[20]. For instance, [2]–[6] considered different interference-limited scenarios with single-antenna transceivers subject to additive hardware distortions (AHWD). When there is AHWD, the distortion power is a linear function of the signal power at the corresponding antenna [2]–[6]. In [2], the authors investigated the effect of AHWD on the performance of a dual-hop relay with both amplify-and-forward and decode-and-forward protocols and derived closed-form expressions for outage

probabilities, as well as an upper bound for the ergodic capacity. The outage probability for a device-to-device mmW communication system with complex proper AHWD was derived in [3]. However, AHWD may be, in general, improper due to I/Q imbalance [4]–[6], [43]–[47]. The authors in [4] considered a relay channel with improper AHWD and maximized the achievable rate of the system by optimizing over complementary variances. In [5], the authors considered a full-duplex multihop relay channel with improper AHWD. The work in [6] considered the SISO 2-user IC with improper AHWD and proposed two suboptimal IGS schemes to obtain the achievable rate region of the SISO 2-user IC.

Hardware nonidealities are even more critical in multiple antenna systems, especially in massive multiple-input, multiple-output (MIMO) communications. In massive MIMO systems, employing low-complexity devices is a must to make the implementation costs affordable, and it has therefore attracted a lot of research [9], [10]. Obviously, low-complexity devices may generate significant HWI, which makes HWI-aware schemes important in upcoming multiple antenna systems.

The performance of various multiple antenna systems with hardware nonidealities has been investigated in many papers (see, e.g., [7]–[18]). For instance, the papers [7]–[9] studied secure communications for massive MIMO systems with AHWD in different scenarios. The paper [10] investigated the impact of AHWD on the performance of cellular communication systems in which the base station employs a massive number of antennas. The papers [11]–[13] studied the performance of massive MIMO systems with AHWD in fading channels in different scenarios. In [14], the authors investigated the system performance of a two-way massive MIMO relay channel with AHWD. In [15], the authors considered beamforming designs for a dual-hop MIMO amplify-and-forward relay channel in the presence of AHWD and analyzed the outage probabilities for the system. In [16], the authors studied the capacity limit and multiplexing gain of MIMO point-to-point systems with AHWD at both transmitter and receiver sides.

In addition to AHWD, there might be other sources of hardware imperfections and impairments

like I/Q imbalance¹. When I/Q imbalance occurs, the received signal can be modeled through a widely linear transformation of the transmitted signal and the aggregated noise. Hence, the received signal can be improper even if the transmitted signal and aggregated noise are proper [44]. It has been shown that IGS can improve the system performance in the presence of improper additive noise [4]–[6], [43]–[47]. For example, it is shown in [45] that IGS is the optimal signaling for a point-to-point single-input, multiple-output (SIMO) system with asymmetric or improper AHWD.

IGS has been used as an interference-management tool in [4], [22]–[39]. It was shown that IGS can improve the performance of different interference-limited systems in terms of several performance metrics. First, IGS with interference alignment can increase the degrees of freedom (DoF) of different ICs [22], [23]. Second, IGS can provide significant gains in terms of achievable rate and/or power/energy-efficiency perspectives when interference is treated as noise [24]–[39]. IGS was considered as an interference management technique for the first time in [22], where it was shown that IGS can increase the DoF of the 3-user IC. The papers [24]–[27] showed the superiority of IGS in the 2-user IC from achievable rate point of view. A robust IGS design for the 2-user IC with imperfect channel state information (CSI) was proposed in [26]. The ergodic rate of IGS and PGS schemes in the 2-user IC with statistical CSI was studied in [27]. The works [28]–[31] investigated performance improvements by IGS in the Z-IC. In [33], the authors showed that IGS can decrease the outage probability of the secondary user (SU) in an overlay cognitive radio (CR) for a given rate target. The work [32] showed that IGS can increase the achievable rate of the SU in an underlay CR (UCR) if the interference link is greater than a threshold. Energy-efficient designs for IGS were proposed in [34] for UCR and in [35] for the SISO K -user IC. In [38], the authors showed superiority of IGS in the MIMO broadcast channel. The paper [39] investigated the performance improvements by IGS in non-orthogonal multiple access systems.

The papers [22]–[39] studied the performance of IGS with ideal devices, which is not a realistic scenario. The papers [4]–[6], [43], [45], [46] consider the performance of IGS with AHWD as

¹In this paper, AHWD noise refers to the model in [2], [6], [7], [9]–[11], [13], [16] in which the power of the AHWD noise is a linear function of the power of the received signal. On the other hand, HWI with I/Q imbalance refers to the model in [44], [47], where the received signal is a function of the widely linear transform of the transmitted signal and noise, and the variance of the noise is fixed and independent of signal powers.

indicated before. However, to the best of our knowledge, there is no work on IGS in interference-limited systems in the presence of HWI with I/Q imbalance.

B. Contribution

This paper considers the effect of HWI including I/Q imbalance in a MIMO K -user IC. To the best of our knowledge, this is the first work to study IGS in the MIMO K -user IC with HWI and I/Q imbalance. In order to model hardware nonidealities, we employ the HWI model in [44]. That is, we assume that the transceivers are not perfect and generate an additive white and proper Gaussian noise. Moreover, we assume that the upconversion (at the transmitter side) or the downconversion (at the receiver side) chains suffer from I/Q imbalance, which makes the received signal a function of the widely linear transform of the transmitted signal and the aggregated noise. Thus, the aggregated noise can be improper, which motivates us to consider IGS.

We investigate the performance of IGS as an interference-management technique in this context. We consider two main performance metrics in this paper: the achievable rate and the energy efficiency (EE). The EE of a user is defined as the ratio of its achievable rate to its total power consumption [48]. We show that IGS can outperform proper Gaussian signaling (PGS) in the MIMO K -user IC with HWI and I/Q imbalance from both achievable rate and energy-efficiency perspectives. We observe that the benefits of IGS decrease with the number of antennas either at the transmitter or receiver sides for a fixed number of users. This is due to the fact that interference can be managed more easily by PGS when there are more resources, and consequently, IGS provides less gain as an interference-management technique. We also observe that, for a fixed number of antennas, the benefits of IGS increase with K . The reason is that the interference level increases with K , and the more interference, the better the performance for IGS. Additionally, our results show that the benefits of IGS increase with the imbalance level. The more improper the noise is, the more benefits can be achieved by IGS.

In this paper, we also define a framework to optimize HWI-aware schemes. The framework can be applied to any optimization problem in which the objective and/or the constraints are linear functions of the achievable rates of users. As examples, we consider different optimization

problems such as achievable rate region, maximum sum-rate, energy efficiency region and global energy efficiency. The global EE of a network is defined as the ratio of the total achievable rate of the network to the total power consumption of the network.

The main idea of our framework is based on the structure of the achievable rate or energy-efficiency functions in interference-limited systems when interference is treated as noise. The capacity of a channel is defined as the difference of the entropy of the received signal and the entropy of the noise at the receiver side [49]. When the noise is Gaussian, the capacity-achieving signaling is Gaussian as well. Moreover, the entropy of Gaussian signals involves a logarithmic function, which is a concave function. As a result, the achievable rate when treating interference as noise (TIN) is a difference of two concave/convex functions. We exploit this feature and employ a majorization-minimization (MM) approach to derive a stationary point of every optimization problem in interference-limited systems with TIN in which the objective function and/or the constraints are linear functions of the rates of users. It is worth mentioning that this optimization approach has already been applied to maximize EE with ideal devices in different scenarios, e.g., [50], [51]. In this paper we extend this approach to include hardware imperfections, and generalize it to other performance metrics and optimization problems.

Our results show that IGS can be beneficial in terms of both performance metrics, i.e., achievable rate and EE. Interestingly, IGS provides more gain in terms of achievable rate than from an EE perspective. This is in line with our previous studies on energy efficient IGS schemes in different scenarios [34], [35]. For instance, in [34], we derived the necessary and sufficient conditions for optimality of IGS in UCR from an EE point of view and showed that these conditions are more restrictive than those obtained when the achievable rate is the performance metric. Moreover, although there are some benefits for IGS in terms of global EE for the MIMO K -user IC, these benefits may be minor. In other words, our numerical results suggest that IGS does not provide a considerable gain in terms of global EE for the MIMO K -user IC.

The main contributions of this paper can be summarized as follows:

- We propose HWI-aware IGS schemes for the MIMO K -user IC. We study two general performance metrics, i.e., the achievable rate and EE and solve four different optimization

problems. We derive a stationary point of the rate region, sum-rate maximization, EE region and global EE maximization problems.

- We define a framework to obtain a stationary point of every optimization problem in which the objective function and/or the constraints are linear functions of the achievable rates. It is worth mentioning that although we do not employ these optimization tools for the first time in the literature, we set in this paper a common framework to tackle all these optimization problems. Note that this framework can be applied to any arbitrary interference-limited system with I/Q imbalance and AHWD as long as interference is treated as noise.
- Our results show that IGS can improve the performance of the MIMO K -user IC with HWI and I/Q imbalance in terms of achievable rate and EE. The benefit of employing IGS increases with K and with the level of impairment for a fixed number of antennas. However, IGS provides minor gains with respect to PGS when the number of antennas grows for a fixed number of users. Additionally, we observe that IGS provides more benefits in terms of achievable rate than from an EE perspective.

C. Paper organization

This paper is organized as follows. In Section II, we present the preliminaries and system model. We define our optimization framework for the MIMO IC with HWI at transceivers in Section III. We solve the optimization problems in Section IV. Finally, Section V provides some numerical examples along with an extensive discussion of them.

II. PRELIMINARIES AND SYSTEM MODEL

A. Real decomposition of a complex system

Consider the following point-to-point MIMO communication system

$$\mathbf{y} = \mathbf{H}\mathbf{x} + \mathbf{n}, \quad (1)$$

where $\mathbf{y} \in \mathbb{C}^{N_R \times 1}$, $\mathbf{x} \in \mathbb{C}^{N_T \times 1}$, $\mathbf{n} \in \mathbb{C}^{N_R \times 1}$, and $\mathbf{H} \in \mathbb{C}^{N_R \times N_T}$ are, respectively, the received signal, transmitted signal, noise vector, and the channel matrix. The real decomposition model for the link is

$$\begin{bmatrix} \Re\{\mathbf{y}\} \\ \Im\{\mathbf{y}\} \end{bmatrix} = \begin{bmatrix} \Re\{\mathbf{H}\} & -\Im\{\mathbf{H}\} \\ \Im\{\mathbf{H}\} & \Re\{\mathbf{H}\} \end{bmatrix} \begin{bmatrix} \Re\{\mathbf{x}\} \\ \Im\{\mathbf{x}\} \end{bmatrix} + \begin{bmatrix} \Re\{\mathbf{n}\} \\ \Im\{\mathbf{n}\} \end{bmatrix}. \quad (2)$$

Assume \mathbf{n} is a random vector with Gaussian distribution as $\mathbf{n} \sim \mathcal{CN}(\mathbf{0}, \mathbf{C}_n)$. The achievable rate of the system is [49]

$$R_k = \frac{1}{2} \log_2 \det(\mathbf{C}_n + \mathbf{H}\mathbf{P}\mathbf{H}^T) - \frac{1}{2} \log_2 \det(\mathbf{C}_n), \quad (3)$$

where \mathbf{C}_n is the covariance matrix of $[\Re\{\mathbf{n}\} \ \Im\{\mathbf{n}\}]^T$, \mathbf{P} is the covariance matrix of $[\Re\{\mathbf{x}\} \ \Im\{\mathbf{x}\}]^T$, and \mathbf{H} is

$$\mathbf{H} = \begin{bmatrix} \Re\{\mathbf{H}\} & -\Im\{\mathbf{H}\} \\ \Im\{\mathbf{H}\} & \Re\{\mathbf{H}\} \end{bmatrix}. \quad (4)$$

B. Preliminaries of IGS

A zero-mean complex Gaussian random variable x with variance $p_x = \mathbb{E}\{|x|^2\}$ is called proper if $\mathbb{E}\{x^2\} = 0$; otherwise, it is improper [40], [41]. When the variable x is improper, its real and imaginary parts are not independent and identically distributed (i.i.d). We can extend the definition of improper scalar variables to vectors. A zero-mean complex Gaussian random vector $\mathbf{x}_{N \times 1}$ with covariance matrix $\mathbf{P}_x = \mathbb{E}\{\mathbf{x}\mathbf{x}^H\}$ is called proper if $\mathbb{E}\{\mathbf{x}\mathbf{x}^T\} = \mathbf{0}$; otherwise, it is improper [40], [41].

To deal with improper signals, there are generally two approaches: augmented covariance matrix [41] and real decomposition method [52]. In the augmented-covariance-matrix approach, complex-domain signals are considered, and the optimized variables are covariance and complementary covariance matrices. However, in the real-decomposition method, every variable is written in the real domain, and the optimization variable is the covariance matrix of the real decomposition of the signals. The main differences of these two approaches are in the structure of the optimization variables as well as corresponding optimization problems. That is, a complementary covariance

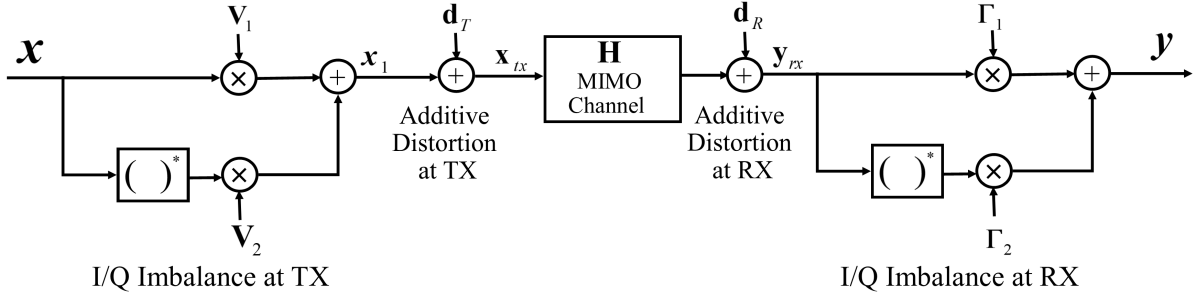


Fig. 1: The transceiver model of a point-to-point communications link with imperfect devices.

matrix has to follow a specific structure for improper signals, while the real covariance matrices are required to be only positive semi-definite. On the one hand, the augmented-covariance-matrix approach can provide insights into the behavior of the signals. For example, we might be able to derive some conditions for optimality of proper or improper signaling by considering complementary variances. On the other hand, depending on the scenario, the optimization over the real domain might be simpler. In this work, we consider the real-decomposition method to simplify the optimization problems.

It is worth emphasizing that, in the real decomposition model, an improper random vector can have any arbitrary symmetric and positive semi-definite covariance matrix. However, a proper Gaussian signal has a covariance matrix with the specific structure [40]

$$\mathbf{P}_x = \mathbb{E} \left\{ \begin{bmatrix} \Re\{\mathbf{x}\} & \Im\{\mathbf{x}\} \end{bmatrix}^T \begin{bmatrix} \Re\{\mathbf{x}\} & \Im\{\mathbf{x}\} \end{bmatrix} \right\} = \begin{bmatrix} \mathbf{A}_{N \times N} & \mathbf{B}_{N \times N} \\ \mathbf{B}_{N \times N}^T & \mathbf{A}_{N \times N} \end{bmatrix}, \quad (5)$$

where \mathbf{A} is symmetric and positive semi-definite, and \mathbf{B} is skew-symmetric, i.e., $\mathbf{B} = -\mathbf{B}^T$, which means its diagonal elements are zero.

C. MIMO hardware imperfection model

In this subsection, we present the MIMO transceiver model with non-ideal devices with N_T transmitter antennas and N_R receiver antennas (see Fig. 1). To this end, we employ the non-ideal-hardware model in [44]. The I/Q imbalance at the transmitter side is modeled as a widely linear

transformation of the transmit signal $\mathbf{x} \in \mathbb{C}^{N_T \times 1}$ as

$$\mathbf{x}_1 = \mathbf{V}_1 \mathbf{x} + \mathbf{V}_2 \mathbf{x}^*, \quad (6)$$

where the matrices $\mathbf{V}_1 \in \mathbb{C}^{N_T \times N_T}$ and $\mathbf{V}_2 \in \mathbb{C}^{N_T \times N_T}$ capture the amplitude and rotational errors and can be expressed as [44]

$$\mathbf{V}_1 = \frac{\mathbf{I}_{N_T} + \mathbf{A}_T e^{j\theta_T}}{2}, \quad (7)$$

$$\mathbf{V}_2 = \mathbf{I}_{N_T} - \mathbf{V}_1^* = \frac{\mathbf{I}_{N_T} - \mathbf{A}_T e^{j\theta_T}}{2}. \quad (8)$$

Moreover, the matrices \mathbf{A}_T and θ_T are diagonal and, respectively, reflect the amplitude and phase errors of each branch at the transmitter side [44]. There is no I/Q imbalance if $\mathbf{A}_T = \mathbf{I}$ and $\theta_T = 0$ or equivalently, $\mathbf{V}_1 = \mathbf{I}$ and $\mathbf{V}_2 = 0$.

We also assume that the transmitter is not perfect and may generate an additive proper Gaussian noise in addition to the I/Q imbalance with probability distribution $\mathbf{d}_T \in \mathbb{C}^{N_T \times 1} \sim \mathcal{CN}(\mathbf{0}, \mathbf{C}_T)$ [44]. Hence, the transmitted signal is

$$\mathbf{x}_{tx} = \mathbf{x}_1 + \mathbf{d}_T. \quad (9)$$

The transmitted signal is delivered to the receiver over a MIMO channel with additive white Gaussian noise. Hence, the received signal is

$$\mathbf{y}_{rx} = \mathbf{H} \mathbf{x}_{tx} + \mathbf{d}_R, \quad (10)$$

where $\mathbf{H} \in \mathbb{C}^{N_R \times N_T}$ is the matrix of the channel coefficients. Moreover, the vector $\mathbf{d}_R \in \mathbb{C}^{N_R \times 1} \sim \mathcal{CN}(\mathbf{0}, \mathbf{C}_R)$ is the aggregate effect of the additive white Gaussian noise of the channel and the additive distortion of the receive devices. The receiver can suffer from an I/Q imbalance similar to the transmitter. Thus, the received signal after I/Q imbalance is

$$\mathbf{y} = \mathbf{\Gamma}_1 \mathbf{y}_{rx} + \mathbf{\Gamma}_2 \mathbf{y}_{rx}^*, \quad (11)$$

where the matrices $\mathbf{\Gamma}_1 \in \mathbb{C}^{N_R \times N_R}$ and $\mathbf{\Gamma}_2 \in \mathbb{C}^{N_R \times N_R}$ are, respectively, given by

$$\mathbf{\Gamma}_1 = \frac{\mathbf{I}_{N_R} + \mathbf{A}_R e^{j\theta_r}}{2} \quad (12)$$

$$\mathbf{\Gamma}_2 = \mathbf{I}_{N_R} - \mathbf{\Gamma}_1^* = \frac{\mathbf{I}_{N_R} - \mathbf{A}_R e^{j\theta_r}}{2}. \quad (13)$$

Similar to \mathbf{A}_T and θ_T , the matrices \mathbf{A}_R and θ_R are diagonal and, respectively, reflect the amplitude and phase errors of each branch at the receiver side [44]. The following lemmas present the aggregate effect of the impairments at the transmitter and receiver sides.

Lemma 1 ([44]). *The transceiver of MIMO system with HWI can be modeled as*

$$\mathbf{y} = \bar{\mathbf{H}}_1 \mathbf{x} + \bar{\mathbf{H}}_2 \mathbf{x}^* + \mathbf{z}, \quad (14)$$

where

$$\bar{\mathbf{H}}_1 = \mathbf{\Gamma}_1 \mathbf{H} \mathbf{V}_1 + \mathbf{\Gamma}_2 \mathbf{H}^* \mathbf{V}_2^* \in \mathbb{C}^{N_R \times N_T}, \quad (15)$$

$$\bar{\mathbf{H}}_2 = \mathbf{\Gamma}_1 \mathbf{H} \mathbf{V}_1 + \mathbf{\Gamma}_2 \mathbf{H}^* \mathbf{V}_2^* \in \mathbb{C}^{N_R \times N_T}, \quad (16)$$

$$\mathbf{z} = \mathbf{\Gamma}_1 (\mathbf{H} \mathbf{d}_T + \mathbf{d}_R) + \mathbf{\Gamma}_2 (\mathbf{H} \mathbf{d}_T + \mathbf{d}_R)^* \in \mathbb{C}^{N_R \times 1}. \quad (17)$$

Proof. Please refer to [44, Lemma 1]. □

Lemma 2. *The real decomposition of the HWI model in Lemma 1 is*

$$\underline{\mathbf{y}} = \tilde{\mathbf{H}} \underline{\mathbf{x}} + \underline{\mathbf{z}}, \quad (18)$$

where $\underline{\mathbf{y}} = \begin{bmatrix} \Re\{\mathbf{y}\} & \Im\{\mathbf{y}\} \end{bmatrix}^T$, $\underline{\mathbf{x}} = \begin{bmatrix} \Re\{\mathbf{x}\} & \Im\{\mathbf{x}\} \end{bmatrix}^T$, and $\underline{\mathbf{z}} = \begin{bmatrix} \Re\{\mathbf{z}\} & \Im\{\mathbf{z}\} \end{bmatrix}^T$ are, respectively, the real decomposition of \mathbf{y} , \mathbf{x} , and \mathbf{z} in (14). Moreover, $\tilde{\mathbf{H}}$ is

$$\tilde{\mathbf{H}} = \begin{bmatrix} \Re\{\bar{\mathbf{H}}_1 + \bar{\mathbf{H}}_2\} & -\Im\{\bar{\mathbf{H}}_1 - \bar{\mathbf{H}}_2\} \\ \Im\{\bar{\mathbf{H}}_1 + \bar{\mathbf{H}}_2\} & \Re\{\bar{\mathbf{H}}_1 - \bar{\mathbf{H}}_2\} \end{bmatrix}. \quad (19)$$

The statistics of the vector $\underline{\mathbf{z}} \in \mathbb{C}^{2N_R \times 1}$ are $\mathbb{E}\{\underline{\mathbf{z}}\} = \mathbf{0}$, and

$$\mathbb{E}\{\underline{\mathbf{z}}\underline{\mathbf{z}}^T\} = \underline{\mathbf{C}}_z = \underline{\mathbf{\Gamma}}\mathbf{C}_d\underline{\mathbf{\Gamma}}^T, \quad (20)$$

where $\mathbf{C}_d = \underline{\mathbf{H}}\underline{\mathbf{C}}_T\underline{\mathbf{H}}^T + \underline{\mathbf{C}}_R$, and

$$\underline{\mathbf{\Gamma}} \triangleq \begin{bmatrix} \Re\{\mathbf{\Gamma}_1 + \mathbf{\Gamma}_2\} & -\Im\{\mathbf{\Gamma}_1 - \mathbf{\Gamma}_2\} \\ \Im\{\mathbf{\Gamma}_1 + \mathbf{\Gamma}_2\} & \Re\{\mathbf{\Gamma}_1 + \mathbf{\Gamma}_2\} \end{bmatrix}. \quad (21)$$

Additionally, $\underline{\mathbf{H}}$, $\underline{\mathbf{C}}_T$, and $\underline{\mathbf{C}}_R$ are, respectively, the real decomposition of \mathbf{H} , \mathbf{C}_T , and \mathbf{C}_R . For example, if $\mathbf{C}_T = \sigma^2 \mathbf{I}_{N_T \times N_T}$, then $\underline{\mathbf{C}}_T = \frac{1}{2}\sigma^2 \mathbf{I}_{2N_T \times 2N_T}$.

Proof. We can easily construct the real decomposition model in (18) from the complex model in (14). Now we would like to derive the statistics of $\underline{\mathbf{z}}$ in (18). To this end, we first write the real decomposition of \mathbf{z} in (17) as

$$\begin{bmatrix} \Re\{\mathbf{z}\} \\ \Im\{\mathbf{z}\} \end{bmatrix} = \begin{bmatrix} \Re\{\mathbf{\Gamma}_1 + \mathbf{\Gamma}_2\} & -\Im\{\mathbf{\Gamma}_1 - \mathbf{\Gamma}_2\} \\ \Im\{\mathbf{\Gamma}_1 + \mathbf{\Gamma}_2\} & \Re\{\mathbf{\Gamma}_1 + \mathbf{\Gamma}_2\} \end{bmatrix} \begin{bmatrix} \Re\{\mathbf{H}\mathbf{d}_T + \mathbf{d}_R\} \\ \Im\{\mathbf{H}\mathbf{d}_T + \mathbf{d}_R\} \end{bmatrix}, \quad (22)$$

which can be represented as $\underline{\mathbf{z}} = \underline{\mathbf{\Gamma}}(\underline{\mathbf{H}}\underline{\mathbf{d}}_T + \underline{\mathbf{d}}_R)$, where $\underline{\mathbf{d}}_T$ and $\underline{\mathbf{d}}_R$ are, respectively, the real decomposition of \mathbf{d}_T and \mathbf{d}_R . The average of $\underline{\mathbf{z}}$ is simply $\mathbf{0}$ since \mathbf{d}_R and \mathbf{d}_T are a zero-mean random vectors. Furthermore, the covariance matrix of $\underline{\mathbf{z}}$ can be derived as (20). □

D. System model

We consider a MIMO K -user IC with imperfect transceivers, as shown in Fig. 2. Without loss of generality, we assume that the transceivers have the same number of antennas and produce a noise with the same statistics to simplify the equations. It is straightforward to extend this model to the most general case with asymmetric devices. According to Lemma 2, the real decomposition of the received signal at the receiver of user k is

$$\underline{\mathbf{y}}_k = \sum_{i=1}^K \tilde{\mathbf{H}}_{ki} \underline{\mathbf{x}}_i + \underline{\mathbf{z}}_k \quad (23)$$

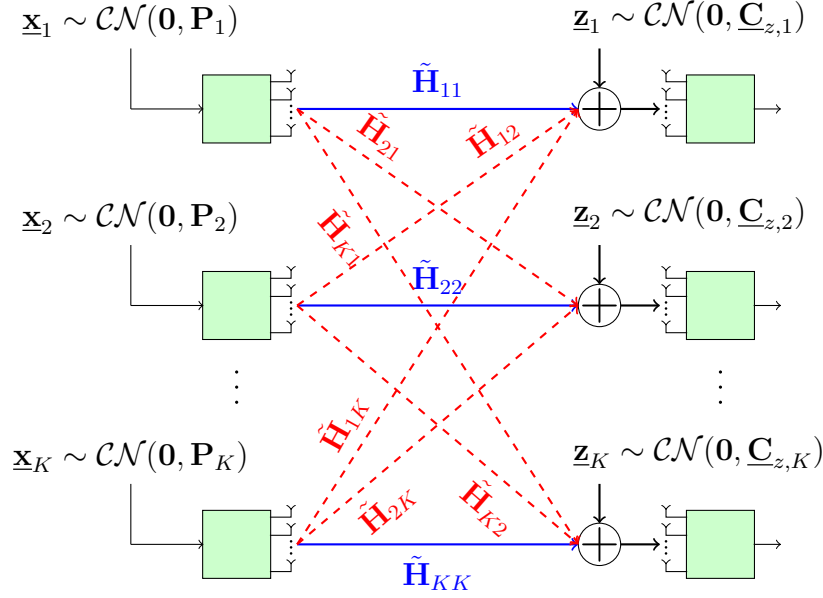


Fig. 2: The equivalent real-decomposition channel model for the MIMO K -user IC.

where $\underline{\mathbf{x}}_i$ is the real decomposition of the transmitted signal of user i , and

$$\tilde{\mathbf{H}}_{ki} = \begin{bmatrix} \Re\{\bar{\mathbf{H}}_{1,ki} + \bar{\mathbf{H}}_{2,ki}\} & -\Im\{\bar{\mathbf{H}}_{1,ki} - \bar{\mathbf{H}}_{2,ki}\} \\ \Im\{\bar{\mathbf{H}}_{1,ki} + \bar{\mathbf{H}}_{2,ki}\} & \Re\{\bar{\mathbf{H}}_{1,ki} - \bar{\mathbf{H}}_{2,ki}\} \end{bmatrix}, \quad (24)$$

where $\bar{\mathbf{H}}_{1,ki}$ and $\bar{\mathbf{H}}_{2,ki}$ can be derived, respectively, by replacing \mathbf{H}_{ki} in (15) and (16). Note that \mathbf{H}_{ki} is the channel matrix for the link between transmitter i and receiver k . Moreover, $\underline{\mathbf{z}}_k$ is the real decomposition of the noise vector \mathbf{z}_k , which is given by

$$\underline{\mathbf{z}}_k = \Gamma_1 \left(\sum_{i=1}^K \mathbf{H}_{ki} \mathbf{d}_{T,i} + \mathbf{d}_{R,k} \right) + \Gamma_2 \left(\sum_{i=1}^K \mathbf{H}_{ki} \mathbf{d}_{T,i} + \mathbf{d}_{R,k} \right)^*. \quad (25)$$

According to Lemma 2, the covariance matrix of $\underline{\mathbf{z}}_k$ is

$$\underline{\mathbf{C}}_{z,k} = \underline{\mathbf{\Gamma}} \left(\sum_{i=1}^K \underline{\mathbf{H}}_{ki} \underline{\mathbf{C}}_T \underline{\mathbf{H}}_{ki}^T + \underline{\mathbf{C}}_R \right) \underline{\mathbf{\Gamma}}^T, \quad (26)$$

where $\underline{\mathbf{H}}_{ki}$ is the real decomposition of \mathbf{H}_{ki} , and $\underline{\mathbf{\Gamma}}$ is given by (21). Treating interference as noise, we can derive the rate of user $k \in \{1, 2, \dots, K\}$ as [40], [49]

$$R_k = \underbrace{\frac{1}{2} \log_2 \det \left(\underline{\mathbf{C}}_{z,k} + \sum_{i=1}^K \tilde{\mathbf{H}}_{ki} \mathbf{P}_i \tilde{\mathbf{H}}_{ki}^T \right)}_{\triangleq r_{k,1}} - \underbrace{\frac{1}{2} \log_2 \det \left(\underline{\mathbf{C}}_{z,k} + \sum_{i=1, i \neq k}^K \tilde{\mathbf{H}}_{ki} \mathbf{P}_i \tilde{\mathbf{H}}_{ki}^T \right)}_{\triangleq r_{k,2}}. \quad (27)$$

As can be observed through (27), the rate of user k is a difference of two concave functions, i.e., $R_k = r_{k,1} - r_{k,2}$, where $r_{k,1}$ and $r_{k,2}$ are concave. This feature allows us to employ majorization minimization (MM) and convex/concave procedure (CCP) for optimization problems in which the objective and/or constraints are linear functions of the rates as will be shown in Section III and Section IV.

III. OPTIMIZATION FRAMEWORK FOR MIMO SYSTEMS BASED MM

In this section, we present a framework based on MM to solve a family of optimization problems in which either the objective function and/or constraints are linear functions of the rates. In this approach, we exploit the fact that the rate is a difference of two concave functions and solve the corresponding optimization problem iteratively. To this end, we apply the CCP to the rates and approximate the convex part of the rates, $-r_{k,2}$, by a linear function through a first-order Taylor expansion.

The proposed framework can be applied to both IGS and PGS schemes. The only difference of IGS and PGS schemes in this framework is the feasibility set of the covariance matrices. As indicated in Section II-B, an improper Gaussian random variable can have an arbitrary symmetric and positive semi-definite covariance matrix. Thus, the feasibility set of the covariance matrices of users $\{\mathbf{P}_k\}_{k=1}^K$ for IGS is

$$\mathcal{P}_{IGS} = \left\{ \{\mathbf{P}_k\}_{k=1}^K : \text{Tr}(\mathbf{P}_k) \leq P_k, \mathbf{P}_k \succcurlyeq \mathbf{0}, k = 1, 2, \dots, K \right\}, \quad (28)$$

where P_k is the power budget of user K . It is in contrast with a proper Gaussian signal, which

has a covariance matrix with the specific structure in (5). In this case, the feasibility set is

$$\mathcal{P}_{PGS} = \left\{ \{\mathbf{P}_k\}_{k=1}^K : \text{Tr}(\mathbf{P}_k) \leq P_k, \mathbf{P}_k = \mathbf{P}_{x_k}, \mathbf{P}_k \succcurlyeq \mathbf{0}, k = 1, 2, \dots, K \right\}, \quad (29)$$

where \mathbf{P}_{x_k} has the structure in (5). In order to include both IGS and PGS schemes in the derivations to follow, we denote the feasibility set of the covariance matrices as \mathcal{P} hereafter.

Consider the following optimization problem

$$\underset{\{\mathbf{P}_k\}_{k=1}^K \in \mathcal{P}}{\text{maximize}} \quad f_0 \left(\{\mathbf{P}_k\}_{k=1}^K \right) \quad \text{s.t.} \quad f_i \left(\{\mathbf{P}_k\}_{k=1}^K \right) \geq 0, \quad i = 1, 2, \dots, I. \quad (30)$$

If $f_0(\cdot)$ and $f_i(\cdot)$ for $i = 1, 2, \dots, I$ are concave, the optimization problem (30) is known to be convex² and can be solved in polynomial time. If $f_0(\cdot)$ and $f_i(\cdot)$ for $i = 1, 2, \dots, I$ are neither concave nor pseudo-concave, it is not straightforward to derive the global optimal solution of (30) in polynomial time [53]–[56]. A way to solve non-convex optimization problems is to employ iterative optimization algorithms such as MM. The MM algorithm consists of two steps at each iteration: majorization and minimization. In the majorization step, the functions $f_0(\cdot)$ and $f_i(\cdot)$ for $i = 1, 2, \dots, I$ are approximated by surrogate functions. Then, the corresponding surrogate problem is solved in the minimization step. In the following lemma, we present convergence conditions of MM iterative algorithms.

Lemma 3 ([53]). *Let us define $\tilde{f}_i^{(l)}(\cdot)$ for $l \in \mathbb{N}$ as surrogate functions of $f_i(\cdot)$ for $i = 0, 1, 2, \dots, I$ such that the following conditions are fulfilled:*

- $\tilde{f}_i^{(l)} \left(\{\mathbf{P}_k^{(l)}\}_{k=1}^K \right) = f_i \left(\{\mathbf{P}_k^{(l)}\}_{k=1}^K \right)$ for $i = 0, 1, 2, \dots, I$.
- $\frac{\partial \tilde{f}_i^{(l)} \left(\{\mathbf{P}_k^{(l)}\}_{k=1}^K \right)}{\partial \mathbf{P}_k} = \frac{\partial f_i \left(\{\mathbf{P}_k^{(l)}\}_{k=1}^K \right)}{\partial \mathbf{P}_k}$ for $i = 0, 1, 2, \dots, I$ and $k = 1, 2, \dots, K$.
- $\tilde{f}_i^{(l)}(\cdot) \leq f_i(\cdot)$ for $i = 0, 1, 2, \dots, I$ for all feasible $\{\mathbf{P}_k\}_{k=1}^K$,

where $\{\mathbf{P}_k^{(l)}\}_{k=1}^K$ is the initial point at the l th iteration of the MM algorithm, which is obtained

²In [53], it is defined as a concave optimization problem. However, we call it convex since such an optimization problem is also widely known as a convex optimization problem [54].

by solving

$$\underset{\{\mathbf{P}_k\}_{k=1}^K \in \mathcal{P}}{\text{maximize}} \quad \tilde{f}_0^{(l-1)}\left(\{\mathbf{P}_k\}_{k=1}^K\right) \quad \text{s.t.} \quad \tilde{f}_i^{(l-1)}\left(\{\mathbf{P}_k\}_{k=1}^K\right) \geq 0, \quad i = 1, 2, \dots, I. \quad (31)$$

Then, the sequence of $\{\mathbf{P}_k^{(l)}\}_{k=1}^K$ converges to a stationary point of (30).

Remark 1. The surrogate optimization problem (31) is not necessarily convex; however, we can obtain the global optimal solution of (31) much more easily than (30).

Note that finding surrogate functions depends on the structure of the objective and constraint functions. In general, there might be different approaches to obtain a surrogate function (see, e.g., [56]). As indicated in Section II-D, the rate of each user is a difference of two concave functions, which allows us to apply CCP to obtain a suitable surrogate function. That is, we approximate the convex part of the rate expressions in (27) by its first-order Taylor series expansion, which is a linear function. By MM and CCP, we are able to obtain a stationary point of different optimization problems in which either the objective or constraint functions are linear functions of the rates of the users, as will be discussed in Section IV. In the following lemmas, we present the surrogate functions for the rates.

Lemma 4. Using CCP, we can obtain an affine upper bound for $\log \det(\mathbf{Q})$ as

$$\log \det(\mathbf{Q}) \leq \log \det(\mathbf{Q}^{(l)}) + \text{Trace}((\mathbf{Q}^{(l)})^{-1}(\mathbf{Q} - \mathbf{Q}^{(l)})), \quad (32)$$

where $\mathbf{Q}^{(l)}$ is any feasible fixed point.

Proof. A concave function can be majorized by an affine function if these two functions have the same value and the same derivative in a point [56]. The logarithmic function is concave. Furthermore, the left-hand and the right-hand sides of (32) hold these condition at $\mathbf{Q} = \mathbf{Q}^{(l)}$. Thus, the upper-bound in (32) holds for all feasible \mathbf{Q} . Note that the derivative of $\log \det(\mathbf{Q})$ with respect to \mathbf{Q} is \mathbf{Q}^{-1} . \square

Lemma 5. *A concave approximation of the rates in (27) can be obtained by CCP as*

$$R_k \geq \tilde{R}_k^{(l)} = r_{k,1} - r_{k,2} \left(\{\mathbf{P}_i^{(l)}\}_{i=1}^K \right) - \text{Tr} \left(\sum_{i=1, i \neq k}^K \frac{\partial r_{k,2} \left(\{\mathbf{P}_i^{(l)}\}_{i=1}^K \right)^T}{\partial \mathbf{P}_i} (\mathbf{P}_i - \mathbf{P}_i^{(l)}) \right) \quad (33)$$

where $r_{k,1}$ and $r_{k,2}$ are, respectively, the concave and convex parts of R_k in (27). Moreover, $\frac{\partial r_{k,2} \left(\{\mathbf{P}_i^{(l)}\}_{i=1}^K \right)}{\partial \mathbf{P}_i}$ is the derivative of $r_{k,2}$ with respect to \mathbf{P}_i at the previous iteration as

$$\frac{\partial r_{k,2} \left(\{\mathbf{P}_i^{(l)}\}_{i=1}^K \right)}{\partial \mathbf{P}_i} = \tilde{\mathbf{H}}_{ki}^T \left(\underline{\mathbf{C}}_{z,k} + \sum_{i=1, i \neq k}^K \tilde{\mathbf{H}}_{ki} \mathbf{P}_i^{(l)} \tilde{\mathbf{H}}_{ki}^T \right)^{-1} \tilde{\mathbf{H}}_{ki}. \quad (34)$$

Note that $r_{k,2} \left(\{\mathbf{P}_i^{(l)}\}_{i=1}^K \right)$ is constant and is given by $r_{k,2}$ at the previous step. Additionally, R_k and $\tilde{R}_k^{(l)}$ fulfill the conditions in Lemma 3.

IV. PROBLEM STATEMENT

In this section, we present a family of optimization problems, which can be solved by the framework described in Section III. In general, any optimization problem in which either the objective or the constraint functions are linear functions of the rates, can be solved by this framework.

A. Achievable rate region

In this subsection, we derive the rate region of the MIMO K -user IC with HWI, which can be cast as [25]

$$\underset{R, \{\mathbf{P}_k\}_{k=1}^K \in \mathcal{P}}{\text{maximize}} \quad R \quad \text{s.t.} \quad R_k \geq \alpha_k R, \quad k = 1, 2, \dots, K, \quad (35)$$

where $\alpha_k \geq 0$ for $k = 1, 2, \dots, K$ are given constants, and $\sum_{k=1}^K \alpha_k = 1$. The boundary of the achievable rate region can be derived by solving (35) for different values of the α_k s. The optimization problem (35) is not convex; however, we can obtain its stationary point by the framework proposed in Section III. That is, we solve (35) iteratively, and in each iteration, we employ the surrogate function in Lemma 5 for the rates. Since the corresponding surrogate

optimization problem is convex, we can efficiently derive the global optimal solution of each surrogate optimization problem and consequently, obtain a stationary point of (35).

B. Maximizing sum-rate

The sum-rate of the MIMO K -user IC with HWI can be obtained by solving

$$\begin{aligned} & \underset{\{\mathbf{P}_k\}_{k=1}^K \in \mathcal{P}}{\text{maximize}} && \sum_{k=1}^K R_k \end{aligned} \quad (36a)$$

$$\text{s.t.} \quad R_k \geq R_{\text{th},k}, \quad k = 1, 2, \dots, K, \quad (36b)$$

where (36b) is the quality of service (QoS) constraint, and $R_{\text{th},k}$ is a given threshold for the rate of user k . Note that the $R_{\text{th},k}$ s have to be set to make (36) feasible. Similar to (35), we can solve (36) by the framework in Section III and obtain its stationary point. Note that each surrogate optimization problem is convex, which can be solved efficiently.

C. Energy-efficiency region

Now we consider the EE of the MIMO K -user IC with HWI. The EE of user k is defined as the ratio of its achievable rate to its power consumption [48]

$$E_k = \frac{R_k}{\eta_k \text{Tr}(\mathbf{P}_k) + P_{c,k}}, \quad (\text{bits/Joule}) \quad (37)$$

where η_k^{-1} , and $P_{c,k}$ are, respectively, the power transmission efficiency of user k , and the constant power consumption of the k th transceiver. The EE function is a linear function of the rates, which allows us to apply the framework in Section III to optimize the EE. EE function has a fractional structure, which makes its optimization more difficult than the rate analysis, as will be discussed in the following.

The EE region of the MIMO K -user IC with HWI can be derived by solving [48]

$$\underset{E, \{\mathbf{P}_k\}_{k=1}^K \in \mathcal{P}}{\text{maximize}} \quad E \quad (38a)$$

$$\text{s.t.} \quad E_k = \frac{R_k}{\eta_k \text{Tr}(\mathbf{P}_k) + P_{c,k}} \geq \alpha_k E, \quad k = 1, 2, \dots, K, \quad (38b)$$

$$R_k \geq R_{\text{th},k}, \quad k = 1, 2, \dots, K, \quad (38c)$$

where $\alpha_k \geq 0$ for $k = 1, 2, \dots, K$ and $\sum_{k=1}^K \alpha_k = 1$. Moreover, the constraint (38c) is the QoS constraint, similar to (36b), and $R_{\text{th},k}$ has to be chosen such that the feasible set of parameters is not empty. Similar to (35), the boundary of the EE region can be derived by solving (38) for all possible α_k s. Since E_k is a linear function of R_k , we can apply the framework in Section III to derive a stationary point of (38). The surrogate optimization problem at the l th iteration is

$$\underset{E, \{\mathbf{P}_k\}_{k=1}^K \in \mathcal{P}}{\text{maximize}} \quad E \quad (39a)$$

$$\text{s.t.} \quad \tilde{E}_k^{(l)} = \frac{\tilde{R}_k^{(l)}}{\eta_k \text{Tr}(\mathbf{P}_k) + P_{c,k}} \geq \alpha_k E, \quad k = 1, 2, \dots, K, \quad (39b)$$

$$\tilde{R}_k^{(l)} \geq R_{\text{th},k}, \quad k = 1, 2, \dots, K. \quad (39c)$$

Note that we can rewrite (39) as a maximin fractional optimization problem by removing E as

$$\max_{\{\mathbf{P}_k\}_{k=1}^K \in \mathcal{P}} \min_{1 \leq k \leq K} \left\{ \frac{\tilde{E}_k^{(l)}}{\alpha_k} \right\} \quad \text{s.t.} \quad \tilde{R}_k^{(l)} \geq R_{\text{th},k}, \quad k = 1, 2, \dots, K. \quad (40)$$

The optimization problem (39) (or equivalently (40)) is not convex; however, its global optimal solution can be derived by employing the generalized Dinkelbach algorithm (GDA). The GDA is a powerful tool to solve maximin fractional optimization problems and is presented in the following Lemma.

Lemma 6. *Consider the following fractional optimization problem*

$$\underset{\{\mathbf{X}\} \in \mathcal{X}}{\text{maximize}} \quad \min_{1 \leq k \leq K} \left\{ \frac{v_k(\mathbf{X})}{u_k(\mathbf{X})} \right\}, \quad (41)$$

where $v_k(\cdot)$ is a concave function in \mathbf{X} , $u_k(\cdot)$ is a convex function in \mathbf{X} , and \mathcal{X} is a compact set. The global optimal solution of (41) can be derived, iteratively, by the GDA, i.e., by solving

$$\begin{aligned} & \underset{t, \{\mathbf{X}\} \in \mathcal{X}}{\text{maximize}} && t && \text{s.t.} && v_k(\mathbf{X}) - \mu^{(m)} u_k(\mathbf{X}) \geq t, && k = 1, 2, \dots, K, \end{aligned} \quad (42)$$

where $\mu^{(m)}$ is constant and given by

$$\mu^{(m)} = \min_{1 \leq k \leq K} \left\{ \frac{v_k(\mathbf{X}^{(m-1)})}{u_k(\mathbf{X}^{(m-1)})} \right\}, \quad (43)$$

where $\mathbf{X}^{(m-1)}$ is the solution of (42) at the $(m-1)$ th iteration. Note that the GDA converges to the global optimal solution of (41) linearly.

Proof. Please refer to [6], [48], [57]. □

Remark 2. In order to apply the GDA, it is not necessary that v_k and $-u_k$ are concave in \mathbf{X} . However, the GDA is ensured to obtain the global optimum solution if v_k and $-u_k$ are concave in \mathbf{X} .

Applying the GDA to (39), we have

$$\underset{E, \{\mathbf{P}_k\}_{k=1}^K \in \mathcal{P}}{\text{maximize}} \quad E \quad (44a)$$

$$\text{s.t.} \quad \tilde{R}_k^{(l)} - \mu^{(m)} (\eta_k \text{Tr}(\mathbf{P}_k) + P_{c,k}) \geq \alpha_k E, \quad k = 1, 2, \dots, K, \quad (44b)$$

$$\tilde{R}_k^{(l)} \geq R_{\text{th},k}, \quad k = 1, 2, \dots, K, \quad (44c)$$

where

$$\mu^{(m)} = \min_{1 \leq k \leq K} \left\{ \frac{E_k \left(\{\mathbf{P}_i^{(l,m-1)}\}_{i=1}^K \right)}{\alpha_k} \right\}, \quad (45)$$

where $\{\mathbf{P}_i^{(l,m-1)}\}_{i=1}^K$ is the solution of (44) at the $(m-1)$ th iteration. Note that the GDA converges to the global optimal solution of (39) linearly, and the whole algorithm converges to a stationary point of (38).

D. Global energy-efficiency

In this subsection, we consider the global EE of the MIMO K -user IC with HWI, which can be cast as [48]

$$\underset{\{\mathbf{P}_k\}_{k=1}^K \in \mathcal{P}}{\text{maximize}} \quad G = \frac{\sum_{k=1}^K R_k}{\sum_{k=1}^K (\eta_k \text{Tr}(\mathbf{P}_k) + P_{c,k})} \quad \text{s.t.} \quad R_k \geq R_{\text{th},k}, \quad k = 1, 2, \dots, K, \quad (46)$$

Similar to (38), since the EE is a linear function of the rates, we can apply the framework in Section III to obtain a stationary point of (46). Thus, the surrogate optimization problem at the l th iteration is

$$\underset{\{\mathbf{P}_k\}_{k=1}^K \in \mathcal{P}}{\text{maximize}} \quad \tilde{G} = \frac{\sum_{k=1}^K \tilde{R}_k}{\sum_{k=1}^K (\eta_k \text{Tr}(\mathbf{P}_k) + P_{c,k})} \quad \text{s.t.} \quad \tilde{R}_k \geq R_{\text{th},k}, \quad k = 1, 2, \dots, K, \quad (47)$$

Similar to (39), the optimization problem is not convex; however, its global optimal solution can be derived by the Dinkelbach algorithm. That is, we obtain $\mathbf{P}_i^{(l,m)}$ by solving

$$\underset{\{\mathbf{P}_k\}_{k=1}^K \in \mathcal{P}}{\text{maximize}} \quad \sum_{k=1}^K \tilde{R}_k - \mu^{(m)} \sum_{k=1}^K (\eta_k \text{Tr}(\mathbf{P}_k) + P_{c,k}) \quad (48a)$$

$$\text{s.t.} \quad \tilde{R}_k \geq R_{\text{th},k}, \quad k = 1, 2, \dots, K, \quad (48b)$$

where $\mu^{(m)} = \tilde{G} \left(\{\mathbf{P}_i^{(l,m-1)}\}_{i=1}^K \right)$, in which $\{\mathbf{P}_i^{(l,m-1)}\}_{i=1}^K$ is the solution of (48) at the $(m-1)$ th iteration. The global optimal solution of (47) can be achieved by iteratively solving (48) and updating $\mu^{(m)}$ until a convergence metric is met. Moreover, as indicated, the whole algorithm converges to a stationary point of (46).

E. Other scenarios

The proposed optimization framework can be applied to many other scenarios, such as orthogonal frequency division multiplexing (OFDM) in which the achievable rate of a user is the summation of the rates of each frequency subband [58]. In this case, the total rate is a difference of two concave functions since the rate of each subband is a difference of two concave functions. As a result, we can apply DCP to derive a stationary point of any optimization problem for multiuser OFDM systems, in which the objective and/or constraints are a linear function of the

total achievable rate. Additionally, we can apply this framework to optimize the rate or the energy efficiency in other interference-limited systems such as underlay cognitive radio, relay channels, broadcast channels, etc. We can also consider more general sources of distortion with arbitrary positive semi-definite covariance matrices.

V. NUMERICAL EXAMPLES

In this section, we provide some numerical examples. We employ Monte Carlo simulations and average the results over 100 channel realizations. In each channel realization, the channel entries are drawn from a zero-mean complex proper Gaussian distribution with unit variance, i.e., $\mathcal{CN}(0, 1)$. For all simulations, the maximum number of the iterations of the MM algorithm is set to 40. We also consider $\mathbf{C}_T = \sigma_T^2 \mathbf{I}_{N_T}$ and $\mathbf{C}_R = \sigma_R^2 \mathbf{I}_{N_R}$ [44], or equivalently $\underline{\mathbf{C}}_T = \frac{1}{2}\sigma_T^2 \mathbf{I}_{2N_T}$ and $\underline{\mathbf{C}}_R = \frac{1}{2}\sigma_R^2 \mathbf{I}_{2N_R}$. In all simulations, we assume $\sigma_T^2 = 0.2$ and $\sigma_R^2 = 1$. We assume that the I/Q imbalance by each antenna is the same. In other words, the matrices $\mathbf{A}_T = a_T \mathbf{I}_{N_T}$, $\boldsymbol{\theta}_T = \phi_T \mathbf{I}_{N_T}$, $\mathbf{A}_R = a_R \mathbf{I}_{N_R}$, and $\boldsymbol{\theta}_R = \phi_R \mathbf{I}_{N_R}$ are scaled identity matrices. We consider $\phi_T = \phi_R = 5$ degrees in all simulations. We also define the signal-to-noise ratio (SNR) as the ratio of the power budget to σ^2 , i.e., $\text{SNR} = \frac{P}{\sigma^2}$.

We compare our proposed algorithms for PGS and IGS with the PGS algorithm for ideal devices. The considered schemes in this section are as follows:

- **IGS:** The IGS scheme.
- **PGS:** The PGS scheme.
- **I-PGS:** The PGS scheme for K -user IC without considering the I/Q imbalance in the design.

It is worth mentioning that the performance of MM algorithms depend on the initial point. In PGS and I-PGS algorithms, we start with a uniform power allocation $\mathbf{P}_k = \frac{P}{2N_t} \mathbf{I}_{2N_t}$ for $k = 1, \dots, K$ in optimization problems (35) and (36) and $\mathbf{P}_k = \frac{0.3P}{2N_t} \mathbf{I}_{2N_t}$ for $k = 1, \dots, K$ in optimization problems (38) and (46). However, the IGS algorithm takes the solution of the PGS algorithm as an initial point.

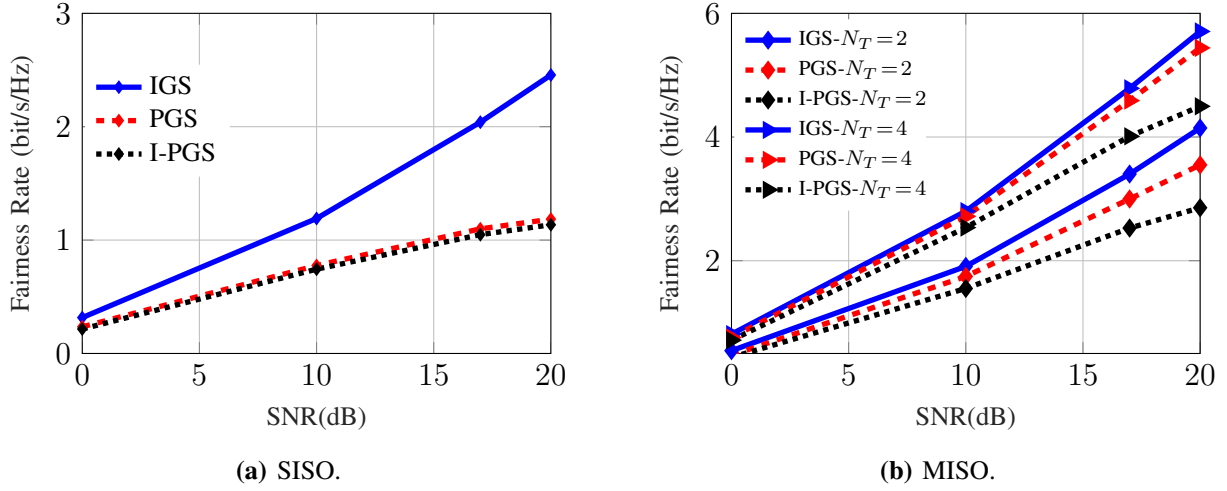


Fig. 3: Fairness rate versus SNR for SISO and MISO.

A. Achievable rate region

In this subsection, we consider a specific point of the rate region, which maximizes the minimum rate of users. The minimum rate of the MIMO K -user IC is maximized for $\alpha_k = \frac{1}{K}$. This point is also referred as the maximin fairness point. Hereafter, we call the minimum rate the fairness rate. We show the fairness rate of the SISO and MISO 2-user IC for $a_T = 0.6$ and different number of antennas at the transmitter side in Fig. 3. As can be observed, there is a huge performance improvement by IGS in the 2-user SISO IC, especially at high SNR. However, the benefits of employing IGS become less substantial when increasing the number of antennas. This is due to the fact that, by increasing the number of spatial resources (e.g. antennas) for a fixed number of users, the interference can be managed more easily, and hence, IGS as an interference management tool does not provide significant gain. This is in line with the results in [58], in which it was shown that IGS might not provide significant benefits in OFDM UCR systems due to the existence of multiple parallel channels over which interference can be managed efficiently without resorting to IGS. Moreover, in [59], it was shown that the IGS does not provide any benefit in comparison to PGS with time sharing when the average power consumption is constrained instead of the *instantaneous power*, which allows a more flexible power allocation. To sum up, the benefits of IGS decrease or even vanish when increasing the number of resources either by increasing

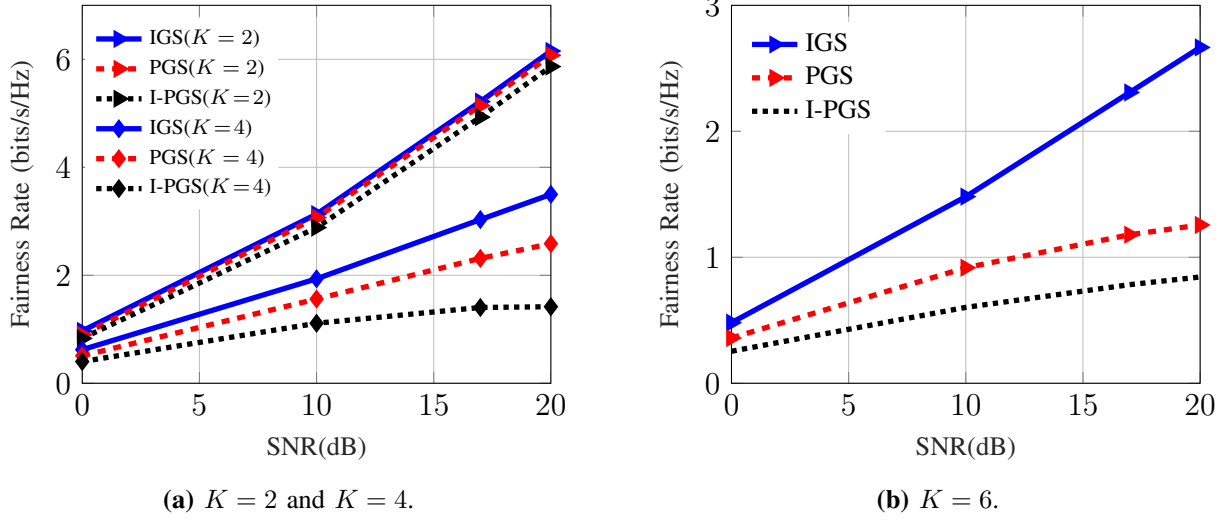


Fig. 4: Fairness rate versus SNR for a 2×2 MIMO.

the number of antennas or number of time slots, by time sharing, and/or the number of parallel channels by OFDM. Nevertheless, it is worth mentioning that, even with many antennas, IGS and HWI-aware PGS outperform PGS, which is designed for ideal devices.

Figure 4 shows the effect of the power budget on the fairness rate of the MIMO K -user IC for $a_T = 0.6$ and $N_T = N_R = 2$. As can be observed, the benefit of IGS is minor when $K = 2$. However, by increasing the number of users, the performance improvement of IGS increases. The reason is that, by increasing the number of users, the interference level increases, which results in more performance improvements by IGS as an interference-management technique. Moreover, IGS performs much better in high SNR for $K = 6$, similar to the SISO 2-user IC as depicted in Fig. 3a.

Figure 5 shows the fairness rate versus the level of the I/Q imbalance, i.e., $1 - a_T$ for SNR = 0 dB and $N_T = N_R = 2$. As can be observed, the IGS design is less affected by the HWI level for different K . When $K = 2$, the IGS and PGS schemes perform very similarly in low HWI level. However, the performance of the PGS scheme drastically decreases with the HWI level, while the fairness rate of the IGS scheme decreases only slightly. When $K = 4$ and $K = 6$, the same behavior is observed, but the relative performance of the IGS scheme over the PGS scheme is

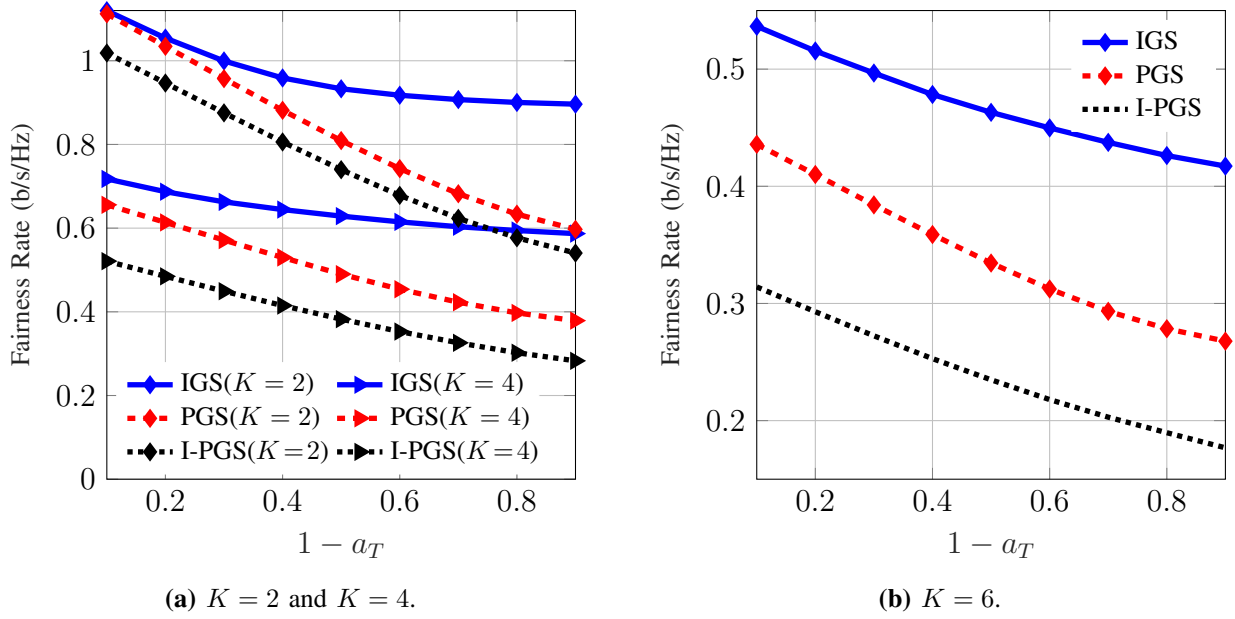


Fig. 5: Fairness rate versus the I/Q imbalance level for a 2×2 MIMO.

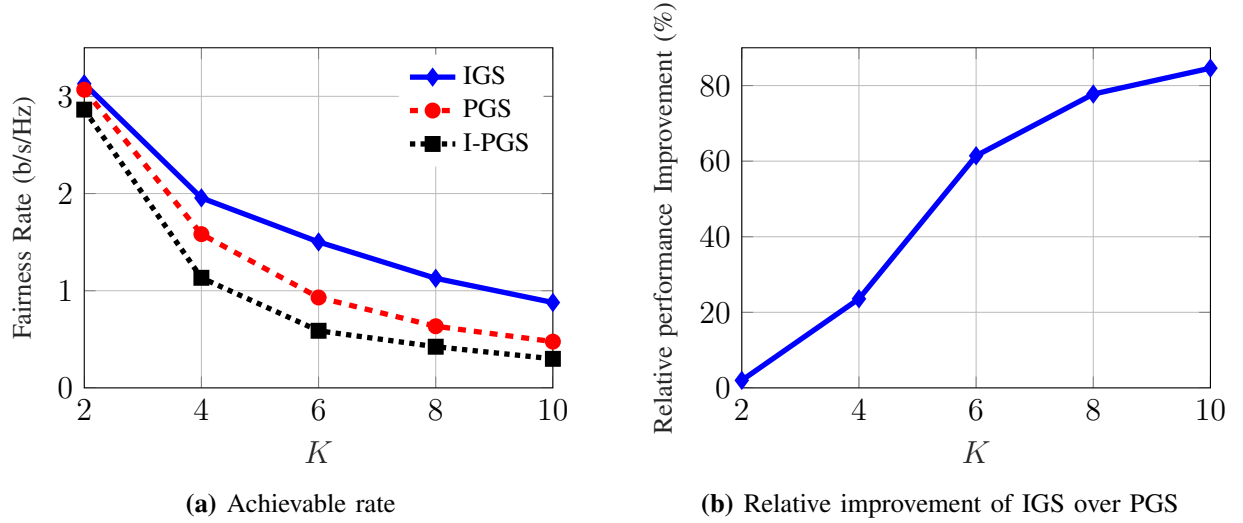
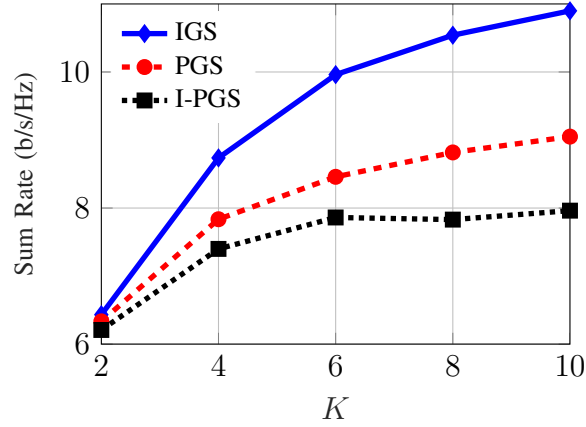


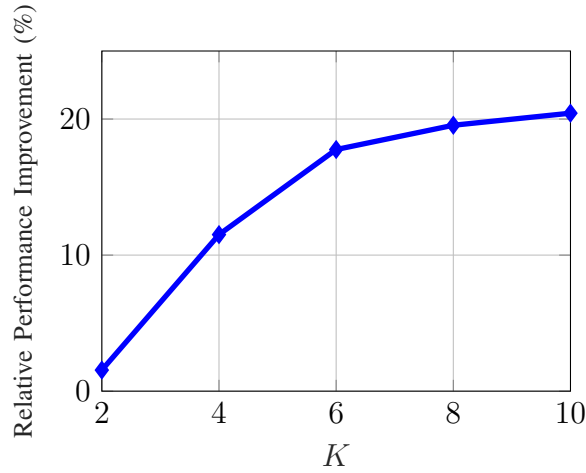
Fig. 6: Fairness rate versus the number of users for a 2×2 MIMO.

increasing with K . Moreover, for a given K , the benefits of IGS increase with the level of the I/Q imbalance, as expected.

Figure 6 considers the effect of the number of users on the fairness rate as well as on the performance of IGS for $\text{SNR} = 10$ dB, $a_T = 0.6$ and $N_T = N_R = 2$. As can be observed, the



(a) Achievable sum-rate



(b) Relative improvement of IGS over PGS

Fig. 7: Achievable sum-rate and relative performance of IGS versus the number of users for a 2×2 MIMO.

fairness rates are related to K^{-1} . Additionally, the relative performance improvement by IGS increases with K , where there is more than 80% improvements over PGS for $K = 10$. The reason is that more users provoke more interference, which results in turn in more improvements by IGS as indicated before.

B. Achievable sum-rate

In Fig. 7, we show the effect of the number of users on the achievable sum-rate of the MIMO K -user IC for SNR= 10 dB, $a_T = 0.6$ and $N_T = N_R = 2$. In this figure, we set the threshold in (36) to $R_{th,k} = 0$. We can observe that the sum-rate and also the relative performance of IGS over

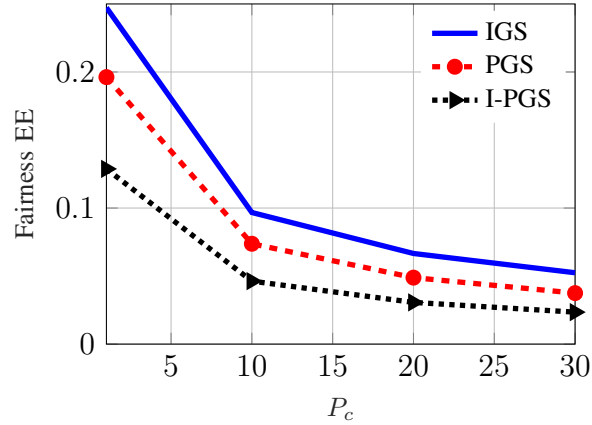


Fig. 8: Symmetric EE of the 2×2 MIMO 6-user IC versus P_c .

PGS are increasing in K . Since we maximize the sum-rate without considering a QoS constraint, the rate of some users with weak direct link might be even 0, which causes less interference. As a result, the relative performance improvement of IGS is less significant than the improvements for the fairness rate observed in Fig. 6.

C. Energy efficiency region

In this subsection, we consider the EE region in (38). In general, IGS provides less EE benefits than rate benefits. For example, in [34], it was shown that there are more constraints for optimality of IGS in an UCR system from an EE point of view than from a rate perspective. In other words, it might happen that IGS provides more rate benefits for the secondary user but, at the same time, PGS is the energy-efficient optimal scheme for the SU.

In Fig. 8, we show the symmetric EE of the MIMO 6-user IC versus P_c for SNR= 10 dB, $a_t = 0.6$ and $N_t = N_r = 2$. As can be observed, the symmetric EE decreases with P_c . Moreover, our proposed IGS scheme outperforms the PGS scheme as well as I-PGS. Figure 9 shows the relative performance improvement by our IGS scheme with respect to the PGS and I-PGS schemes for the results in Fig. 8. As can be observed in these figures, the symmetric EE decreases with P_c ; however, the benefits of employing IGS is increasing in P_c . The reason is that when P_c is very large, the EE-region-optimization problem is simplified to the achievable-rate-region problem, and

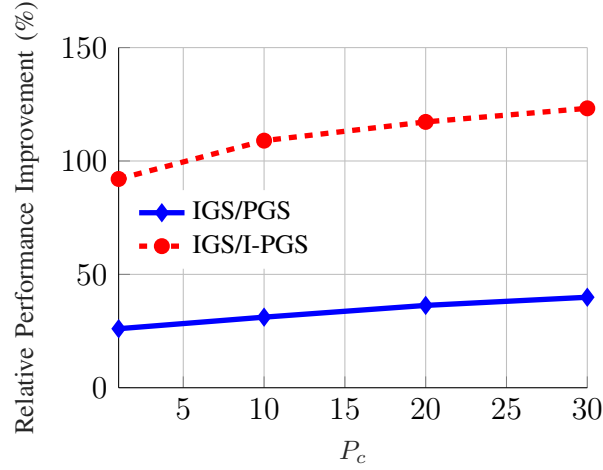


Fig. 9: Relative performance of IGS with respect to PGS and I-PGS versus P_c for the 2×2 MIMO 6-user IC.

as indicated, IGS can provide more gain in achievable-rate optimizations.

D. Global Energy efficiency

Figure 10 shows the global EE of the 2×2 MIMO 6-user IC versus P_c for SNR= 10 dB, $a_t = 0.6$ and $N_t = N_r = 2$. In this figure, we assume $R_{th,k} = 0$ in (46). As can be observed, IGS provides minor benefits for the global EE. Since the QoS constraint is not considered, it might happen that some users are switched off, thus reducing the total level of interference. Moreover, the lower the interference level, the less need for interference-management techniques. Thus, we can expect that the benefits of employing IGS decrease in global EE with respect to EE.

VI. CONCLUSION

This paper studied the effect of HWI with I/Q imbalance at the transceiver of a MIMO K -user IC. In the presence of I/Q imbalance, the received signal is a function of the widely linear transform of the transmitted signal and the aggregated noise. Hence, the effective noise is modeled as improper at the receiver side, which motivated us to consider the use of IGS. Considering achievable rates and EE as performance metrics, we proposed HWI-aware IGS schemes for the MIMO K -user IC. We defined an optimization framework, which can obtain a stationary point of any optimization problem for interference-limited systems with TIN in which the objective

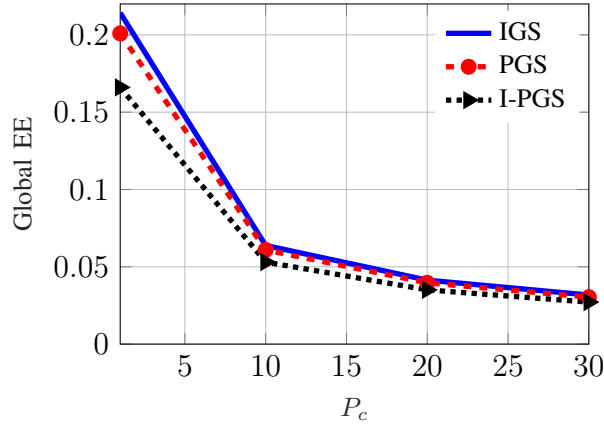


Fig. 10: Global EE of the 2×2 MIMO 6-user IC versus P_c .

function and/or constraints are linear functions of the achievable rate. In this paper, we derived a stationary point of the achievable rate-region, sum-rate maximization, EE region and global EE maximization problems. We observed that the benefits of IGS as an interference-management technique increase with the number of users and decrease with number of antennas. This is due to the fact that higher interference levels result in an increased need for interference management and consequently, more improvements by IGS. We also observed that the benefit of employing IGS increases with impairment level.

As future work, it may be interesting to find out how close the solution of this algorithm is to the corresponding global optimum solutions. Additionally, our scheme is a centralized approach, which might not be applicable in some practical scenarios. Hence, distributed algorithms should also be developed.

ACKNOWLEDGMENTS

This work was supported by the German Research Foundation (DFG) under grants SCHR 1384/7-1 and SCHR 1384/8-1. The work of I. Santamaria was supported by MINECO of Spain and AEI/FEDER funds of the E.U., under grant TEC2016-75067-C4-4-R (CARMEN). The authors would like to thank Dr. C. Lameiro for discussions on the numerical results.

REFERENCES

- [1] R. W. Heath, N. Gonzalez-Prelcic, S. Rangan, W. Roh, and A. M. Sayeed, "An overview of signal processing techniques for millimeter wave MIMO systems," *IEEE J. Sel. Topics Signal Process.*, vol. 10, no. 3, pp. 436–453, 2016.
- [2] E. Bjornson, M. Matthaiou, and M. Debbah, "A new look at dual-hop relaying: Performance limits with hardware impairments," *IEEE Trans. Commun.*, vol. 61, no. 11, pp. 4512–4525, 2013.
- [3] L. Tlebaldiyeva, B. Maham, and T. A. Tsiftsis, "Device-to-device mmwave communication in the presence of interference and hardware distortion noises," *IEEE Commun. Lett.*, 2019.
- [4] S. Javed, O. Amin, and M.-S. Alouini, "Full-duplex relaying under I/Q imbalance using improper Gaussian signaling," in *Proc. IEEE Int. Conf. on Acoust., Speech and Signal Processing (ICASSP)*, 2017, pp. 6538–6542.
- [5] S. Javed, O. Amin, B. Shihada, and M.-S. Alouini, "Improper Gaussian signaling for hardware impaired multihop full-duplex relaying systems," *IEEE Trans. Commun.*, vol. 67, no. 3, pp. 1858–1871, 2019.
- [6] M. Soleymani, C. Lameiro, I. Santamaria, and P. J. Schreier, "Improper signaling for SISO two-user interference channels with additive asymmetric hardware distortion," *IEEE Trans. Commun.*, 2019.
- [7] E. Boshkovska, D. W. K. Ng, L. Dai, and R. Schober, "Power-efficient and secure WPCNs with hardware impairments and non-linear EH circuit," *IEEE Trans. Commun.*, vol. 66, no. 6, pp. 2642–2657, 2018.
- [8] X. Zhang, D. Guo, K. An, and B. Zhang, "Secure communications over cell-free massive MIMO networks with hardware impairments," *IEEE Systems Journal*, 2019.
- [9] J. Zhu, D. W. K. Ng, N. Wang, R. Schober, and V. K. Bhargava, "Analysis and design of secure massive MIMO systems in the presence of hardware impairments," *IEEE Trans. Wireless Commun.*, vol. 16, no. 3, pp. 2001–2016, 2017.
- [10] E. Björnson, J. Hoydis, M. Kountouris, and M. Debbah, "Massive MIMO systems with non-ideal hardware: Energy efficiency, estimation, and capacity limits," *IEEE Trans. Inf. Theory*, vol. 60, no. 11, pp. 7112–7139, 2014.
- [11] J. Zhang, L. Dai, X. Zhang, E. Björnson, and Z. Wang, "Achievable rate of Rician large-scale MIMO channels with transceiver hardware impairments," *IEEE Trans. Veh. Technol.*, vol. 65, no. 10, pp. 8800–8806, 2016.
- [12] Q. Zhang, T. Q. Quek, and S. Jin, "Scaling analysis for massive MIMO systems with hardware impairments in Rician fading," *IEEE Trans. Wireless Commun.*, vol. 17, no. 7, pp. 4536–4549, 2018.
- [13] X. Xia, D. Zhang, K. Xu, W. Ma, and Y. Xu, "Hardware impairments aware transceiver for full-duplex massive MIMO relaying," *IEEE Trans. Signal Process.*, vol. 63, no. 24, pp. 6565–6580, 2015.
- [14] J. Feng, S. Ma, S. Aissa, and M. Xia, "Two-way massive MIMO relaying systems with non-ideal transceivers: Joint power and hardware scaling," *IEEE Trans. Commun.*, 2019.
- [15] S. Cheng, R. Wang, J. Wu, W. Zhang, and Z. Fang, "Performance analysis and beamforming designs of MIMO AF relaying with hardware impairments," *IEEE Trans. Veh. Technol.*, vol. 67, no. 7, pp. 6229–6243, 2018.
- [16] E. Bjornson, P. Zetterberg, M. Bengtsson, and B. Ottersten, "Capacity limits and multiplexing gains of MIMO channels with transceiver impairments," *IEEE Commun. Lett.*, vol. 17, no. 1, pp. 91–94, 2013.
- [17] J. Zhang, Y. Wei, E. Björnson, Y. Han, and S. Jin, "Performance analysis and power control of cell-free massive MIMO systems with hardware impairments," *IEEE Access*, vol. 6, pp. 55 302–55 314, 2018.

- [18] T. Younas, J. Li, and J. Arshad, "On bandwidth efficiency analysis for LS-MIMO with hardware impairments," *IEEE Access*, vol. 5, pp. 5994–6001, 2017.
- [19] G. Mohamed, "Massive relaying communication system under I/Q imbalance and hardware manufacturing problems," *IEEE Systems Journal*, 2019.
- [20] L. Tlebaldiyeva, T. A. Tsiftsis, and B. Maham, "Performance analysis of improved energy detector with hardware impairments for accurate spectrum sensing," *IEEE Access*, vol. 7, pp. 13 927–13 938, 2019.
- [21] J. G. Andrews, S. Buzzi, W. Choi, S. V. Hanly, A. Lozano, A. C. Soong, and J. C. Zhang, "What will 5G be?" *IEEE J. Sel. Areas Commun.*, vol. 32, no. 6, pp. 1065–1082, 2014.
- [22] V. R. Cadambe, S. A. Jafar, and C. Wang, "Interference alignment with asymmetric complex signaling—Settling the Høst-Madsen-Nosratinia conjecture," *IEEE Trans. Inf. Theory*, vol. 56, no. 9, pp. 4552–4565, 2010.
- [23] L. Yang and W. Zhang, "Interference alignment with asymmetric complex signaling on MIMO X channels," *IEEE Trans. Commun.*, vol. 62, no. 10, pp. 3560–3570, 2014.
- [24] Z. K. Ho and E. Jorswieck, "Improper Gaussian signaling on the two-user SISO interference channel," *IEEE Trans. Wireless Commun.*, vol. 11, no. 9, pp. 3194–3203, 2012.
- [25] Y. Zeng, C. M. Yetis, E. Gunawan, Y. L. Guan, and R. Zhang, "Transmit optimization with improper Gaussian signaling for interference channels," *IEEE Trans. Signal Process.*, vol. 61, no. 11, pp. 2899–2913, 2013.
- [26] M. Soleymani, C. Lameiro, I. Santamaria, and P. J. Schreier, "Robust improper signaling for two-user SISO interference channels," *IEEE Trans. Commun.*, vol. 67, no. 7, pp. 4709–4723, 2019.
- [27] M. Soleymani, I. Santamaria, C. Lameiro, and P. J. Schreier, "Ergodic rate for fading interference channels with proper and improper Gaussian signaling," *Entropy*, vol. 21, no. 10, p. 922, 2019.
- [28] H. D. Nguyen, R. Zhang, and S. Sun, "Improper signaling for symbol error rate minimization in K -user interference channel," *IEEE Trans. Commun.*, vol. 63, no. 3, pp. 857–869, 2015.
- [29] S. Lagen, A. Agustin, and J. Vidal, "On the superiority of improper Gaussian signaling in wireless interference MIMO scenarios," *IEEE Trans. Commun.*, vol. 64, no. 8, pp. 3350–3368, 2016.
- [30] E. Kurniawan and S. Sun, "Improper Gaussian signaling scheme for the Z-interference channel," *IEEE Trans. Wireless Commun.*, vol. 14, no. 7, pp. 3912–3923, 2015.
- [31] C. Lameiro, I. Santamaría, and P. J. Schreier, "Rate region boundary of the SISO Z-interference channel with improper signaling," *IEEE Trans. Commun.*, vol. 65, no. 3, pp. 1022–1034, 2017.
- [32] —, "Benefits of improper signaling for underlay cognitive radio," *IEEE Wireless Commun. Lett.*, vol. 4, no. 1, pp. 22–25, 2015.
- [33] O. Amin, W. Abediseid, and M.-S. Alouini, "Overlay spectrum sharing using improper Gaussian signaling," *IEEE J. Sel. Areas Commun.*, vol. 35, no. 1, pp. 50–62, 2017.
- [34] M. Soleymani, C. Lameiro, P. J. Schreier, and I. Santamaria, "Energy-efficient design for underlay cognitive radio using improper signaling," in *Proc. IEEE Int. Conf. on Acoust., Speech and Signal Processing (ICASSP)*, 2019, pp. 4769–4773.
- [35] M. Soleymani, C. Lameiro, I. Santamaria, and P. J. Schreier, "Energy-Efficient improper signaling for K -User interference channels," in *Proc. IEEE European Signal Processing Conference (EUSIPCO)*, 2019.

- [36] S. Lagen, A. Agustin, and J. Vidal, "Coexisting linear and widely linear transceivers in the MIMO interference channel," *IEEE Trans. Signal Process.*, vol. 64, no. 3, pp. 652–664, 2016.
- [37] M. Gaafar, O. Amin, W. Abediseid, and M.-S. Alouini, "Underlay spectrum sharing techniques with in-band full-duplex systems using improper Gaussian signaling," *IEEE Trans. Wireless Commun.*, vol. 16, no. 1, pp. 235–249, 2017.
- [38] A. A. Nasir, H. D. Tuan, T. Q. Duong, and H. V. Poor, "Improper Gaussian signaling for broadcast interference networks," *IEEE Signal Process. Lett.*, vol. 26, no. 6, pp. 808–812, 2019.
- [39] H. D. Tuan, A. A. Nasir, H. H. Nguyen, T. Q. Duong, and H. V. Poor, "Non-orthogonal multiple access with improper Gaussian signaling," *IEEE J. Sel. Topics Signal Process.*, vol. 13, no. 3, pp. 496–507, 2019.
- [40] P. J. Schreier and L. L. Scharf, *Statistical Signal Processing of Complex-Valued Data: the Theory of Improper and Noncircular Signals*. Cambridge University Press, 2010.
- [41] T. Adali, P. J. Schreier, and L. L. Scharf, "Complex-valued signal processing: The proper way to deal with impropriety," *IEEE Trans. Signal Process.*, vol. 59, no. 11, pp. 5101–5125, 2011.
- [42] T. Adali and P. J. Schreier, "Optimization and estimation of complex-valued signals: Theory and applications in filtering and blind source separation," *IEEE Signal Process. Mag.*, vol. 31, no. 5, pp. 112–128, 2014.
- [43] S. Javed, O. Amin, S. S. Ikki, and M.-S. Alouini, "Asymmetric modulation for hardware impaired systems-error probability analysis and receiver design," *IEEE Trans. Wireless Commun.*, vol. 18, no. 3, pp. 1723–1738, 2019.
- [44] —, "Multiple antenna systems with hardware impairments: New performance limits," *IEEE Trans. Veh. Technol.*, vol. 68, no. 2, pp. 1593–1606, 2019.
- [45] —, "Asymmetric hardware distortions in receive diversity systems: Outage performance analysis," *IEEE Access*, vol. 5, pp. 4492–4504, 2017.
- [46] —, "Impact of improper Gaussian signaling on hardware impaired systems," in *Proc. IEEE Int. Conf. Commun. (ICC)*, 2017, pp. 1–6.
- [47] A.-A. A. Boulogeorgos, N. D. Chatzidiamantis, and G. K. Karagiannidis, "Energy detection spectrum sensing under RF imperfections," *IEEE Trans. Wireless Commun.*, vol. 64, no. 7, pp. 2754–2766, 2016.
- [48] A. Zappone and E. Jorswieck, "Energy efficiency in wireless networks via fractional programming theory," *Found Trends[®] in Commun. Inf. Theory*, vol. 11, no. 3-4, pp. 185–396, 2015.
- [49] T. M. Cover and J. A. Thomas, *Elements of Information Theory*. John Wiley & Sons, 2012.
- [50] A. Zappone, P.-H. Lin, and E. A. Jorswieck, "Secrecy energy efficiency for MIMO single-and multi-cell downlink transmission with confidential messages," *IEEE Trans. Inf. Forensics Security*, vol. 14, no. 8, pp. 2059–2073, 2019.
- [51] A. Zappone, P.-H. Lin, and E. Jorswieck, "Optimal energy-efficient design of confidential multiple-antenna systems," *IEEE Trans. Inf. Forensics Security*, vol. 13, no. 1, pp. 237–252, 2017.
- [52] C. Hellings and W. Utschick, "Block-skew-circulant matrices in complex-valued signal processing," *IEEE Trans. Signal Process.*, vol. 63, no. 8, pp. 2093–2107, 2015.
- [53] A. Aubry, A. De Maio, A. Zappone, M. Razaviyayn, and Z.-Q. Luo, "A new sequential optimization procedure and its applications to resource allocation for wireless systems," *IEEE Trans. Signal Process.*, vol. 66, no. 24, pp. 6518–6533, 2018.
- [54] S. Boyd and L. Vandenberghe, *Convex Optimization*. Cambridge University Press, 2004.

- [55] Y. Yang and M. Pesavento, "A unified successive pseudoconvex approximation framework," *IEEE Trans. Signal Process.*, vol. 65, no. 13, pp. 3313–3328, 2017.
- [56] Y. Sun, P. Babu, and D. P. Palomar, "Majorization-minimization algorithms in signal processing, communications, and machine learning," *IEEE Trans. Signal Process.*, vol. 65, no. 3, pp. 794–816, 2017.
- [57] J.-P. Crouzeix and J. A. Ferland, "Algorithms for generalized fractional programming," *Math. Programm.*, vol. 52, no. 1-3, pp. 191–207, May 1991.
- [58] M. Soleymani, C. Lameiro, P. J. Schreier, and I. Santamaria, "Improper signaling for OFDM underlay cognitive radio systems," in *2018 IEEE Statistical Signal Process. Workshop (SSP)*. IEEE, 2018, pp. 722–726.
- [59] C. Hellings and W. Utschick, "Improper signaling versus time-sharing in the two-user Gaussian interference channel with TIN," *arXiv preprint arXiv:1808.01611*, 2018.